

*Work performed under the auspices of the U. S. Atomic Energy Commission.

¹T. Lauritsen and F. Ajzenberg-Selove, Nucl. Phys. **78**, 1 (1966).

²Y. S. Chen, T. A. Tombrello, and R. W. Kavanagh, Nucl. Phys. **A146**, 136 (1970); B. E. F. Macefield, B. Wakefield, and D. H. Wilkinson, *ibid.* **A131**, 250 (1969).

³For example, I. Dostrovsky, R. Davis, Jr., A. M. Poskanzer, and P. L. Reeder, Phys. Rev. **139**, B1513 (1965).

⁴R. Middleton and D. J. Pullen, Nucl. Phys. **51**, 50 (1964); also see J. R. Rook, *ibid.* **55**, 523 (1964).

⁵P. H. Nettles, D. C. Hensley, and T. A. Tombrello, in *Proceedings of the Second Conference on Nuclear Isospin, Asilomar-Pacific Grove, California, March 1969*, edited by J. D. Anderson, S. D. Bloom, J. Cerny, and W. W. True (Academic, New York, 1969), p. 819.

⁶J. C. Hardy, R. I. Verrall, R. Barton, and R. E. Bell, Phys. Rev. Letters **14**, 376 (1965).

⁷G. F. Trentelman, B. M. Preedom, and E. Kashy, Phys. Rev. Letters **25**, 530 (1970); J. Cerny, R. H. Pehl, F. S. Goulding, and D. A. Landis, *ibid.* **13**, 726 (1964).

⁸C. A. Barnes, E. G. Adelberger, D. C. Hensley, and A. B. MacDonald, in *Proceedings of the International Conference on Nuclear Physics, Gallinburg, Tennessee, September 1966*, edited by R. L. Becker, C. D. Goodman, P. H. Stelson, and A. Zucker (Academic, New York, 1967), p. 261; J. M. Mosher, R. W. Kavanagh, and T. A. Tombrello, Phys. Rev. **C 3**, 438 (1971).

⁹G. C. Ball and J. Cerny, Phys. Rev. **177**, 1466 (1969).

¹⁰J. C. Hardy, J. M. Loiseaux, J. Cerny, and G. T. Garvey, Nucl. Phys. **A162**, 552 (1971).

¹¹J. C. Adloff, K. H. Souw, and C. L. Cocke, Phys. Rev. **C 3**, 1808 (1971).

¹²G. M. Griffiths, Nucl. Phys. **65**, 647 (1965).

¹³B. Lynch, G. M. Griffiths, and T. Lauritsen, Nucl. Phys. **65**, 641 (1965); C. L. Cocke, *ibid.* **A110**, 321 (1968).

¹⁴F. Ajzenberg-Selove and R. D. Wardaski, J. Phys. Soc. Japan, Suppl. **24**, 108 (1968).

¹⁵H. G. Clerc, K. H. Wetzel, and E. Spamer, Phys. Letters **20**, 667 (1966).

¹⁶J. B. Woods and D. H. Wilkinson, Nucl. Phys. **61**, 661 (1965).

¹⁷W. L. Imhof, L. F. Chase, Jr., and D. B. Fossan, Phys. Rev. **139**, B904 (1965).

¹⁸S. Cohen and D. Kurath, Nucl. Phys. **73**, 1 (1965); **A141**, 145 (1970); E. C. Halbert, Y. E. Kim, and T. T. S. Kuo, Phys. Letters **20**, 657 (1966).

¹⁹F. C. Barker, Nucl. Phys. **83**, 418 (1966).

²⁰J. L. Norton and P. Goldhammer, Nucl. Phys. **A165**, 33 (1971).

²¹R. H. Stokes and P. G. Young, Phys. Rev. **178**, 1789 (1969).

²²R. M. Drisko, private communication.

²³R. N. Glover and A. D. W. Jones, Nucl. Phys. **81**, 268 (1966).

²⁴R. G. Summers-Gill, Phys. Rev. **109**, 1591 (1958).

²⁵F. C. Barker, private communication.

Resonance Structure in Reaction ${}^9\text{Be}(d, \gamma){}^{11}\text{B}^\dagger$

K. Battleson* and D. K. McDaniels

Department of Physics, University of Oregon, Eugene, Oregon 97403

(Received 9 August 1971)

The reaction ${}^9\text{Be}(d, \gamma){}^{11}\text{B}$ has been studied over the deuteron energy range of 0.56–3.56 MeV. A pulsed deuteron beam and time-of-flight electronics have been utilized to separate deuteron-capture γ rays from events due to neutrons and cosmic rays. From a graphical analysis of the excitation functions for the ground, first, and combined second and third excited states, two resonances have been identified corresponding to ${}^{11}\text{B}$ excitation energies of 17.44 ± 0.05 and 18.37 ± 0.05 MeV. The first of these occurs at the same energy as a level in ${}^{11}\text{B}$ found from other reactions. An interpretation in terms of $1s_{1/2}$ hole states is suggested. The overall behavior of the three excitation functions is used to justify a direct-capture reaction mechanism. Angular distributions were measured at 21 different deuteron energies. The near symmetry of the angular distributions about 90° and the peaking at 90° imply that a one-step deuteron-capture process is important for this reaction if the direct-capture mechanism is dominant. An appreciable forward peaking is observed for the first-excited-state angular distribution.

I. INTRODUCTION

The study of the radiative capture of energetic nucleons and composite particles has been undertaken primarily to understand the basic reaction mechanism. The capture of nucleons with an incident energy of less than a few MeV is adequately

described by the compound-nucleus model. However, it has been definitely established that the capture of higher-energy neutrons and protons cannot be explained by statistical theory calculations.^{1,2} Two types of direct-capture theories have been proposed. In the simplest of these, the incident nucleon is pictured as making a transition from a

single-particle state of the optical potential for it and the target nucleus to a single-particle level of the residual nucleus.³⁻⁶ The failure of this picture to adequately describe the magnitude of the capture cross section of nucleons with an energy between 5 and 25 MeV⁷ caused a semidirect model to be proposed.⁸⁻¹⁰ This model pictures the nucleon making a transition in its optical potential which excites the target nucleus into its giant dipole resonance as an intermediate state. The resulting enhancement of the radiative-capture cross sections has brought both theory and experiment into substantial agreement.^{11, 12}

The capture of composite particles is by no means as well understood. The measurements of the radiative-capture cross sections for α particles of an energy of 5–50 MeV seem to be well described by statistical theory calculations, particularly when corrections for multiple γ -ray cascades and angular momentum effects are included.¹³ For deuterons, the relative importance of the compound-nuclear and direct-capture processes has not yet been satisfactorily established, owing primarily to a lack of good data. Myerhof *et al.* from an analysis of the shape of the $D(d, \gamma)^4\text{He}$ cross section from 6- to 19-MeV deuteron energy concluded that a direct-reaction mechanism was dominant.¹⁴ A study of the uranium isotopes also favored the direct-capture process.¹⁵ However, statistical theory calculations using different methods of evaluating level densities^{13, 16} obtained rough agreement with the (d, γ) data on ^{30}Si and ^{138}Ba for 4–15-MeV deuterons.¹⁶ Similar agreement with the compound-nuclear predictions was obtained for ^{54}Cr , ^{58}Ni , and ^{64}Zn targets.¹⁷

The (d, γ) reaction can also be investigated using information from the photodeuteron reaction and the principle of detailed balance. Madsen and Henley¹⁸ have made an extensive theoretical investigation of this reaction. They find that, while the direct electric dipole ejection of a deuteron is small for all but light nuclei because of the $[(N-Z)/A]$ effective-charge factor, a two-step process in which a nucleon is first excited and then picks up another nucleon in a relative S state to form a deuteron, can be important. The standard technique in the study of the (γ, d) reaction is to measure deuteron/proton yield ratios and calculate the deuteron cross section from the known proton cross section. Chizov *et al.*¹⁹ measured a $(\gamma, d)/(\gamma, p)$ yield ratio (for particles of energy greater than 15 MeV) for targets covering a wide range of A . Yield ratios of the order of several percent for 90-MeV bremsstrahlung with strongly forward-peaked angular distributions for the emitted deuterons were found. The compound-nuclear reaction mechanism failed to explain

these results. Instead, the two-step mechanism was invoked to explain the dependence of the yield measurements on mass number. For light nuclei, the possibility of direct ejection could not be ruled out.

Three previous investigations of the reaction $^9\text{Be}(d, \gamma)^{11}\text{B}$ have been reported. The earliest study using a threshold detector²⁰ obtained an upper limit of $1.8 \mu\text{b}$ for the cross section at 0.90 MeV. Ziegler, Buss, and Waffler (ZBW)²¹ measured the ground-state excitation function over the deuteron energy range of 0.4–1.4 MeV. A peak value of $4.0 \pm 0.8 \mu\text{b}$ was obtained at $E_d = 1.1$ MeV, showing the inaccuracy of the early result. No structure was found in the measured ground-state excitation function. From the observed intensity ratios for transitions to the ground state, first excited state, and the combined second and third excited states, these authors concluded that the basic reaction mechanism was that of direct capture. Suffert²² studied only the ground-state transition, but covered the energy region from 0.5 to 5.3 MeV. His peak cross section occurred at about 1.1 MeV, in agreement with ZBW,²¹ but a value of $7.8 \pm 3.5 \mu\text{b}$ was obtained. His excitation function showed a relatively smooth decrease from $E_d = 1.1$ to 5.3 MeV, although there were a few anomalous data points, and the statistical accuracy was only about 8–10%. Angular distributions were measured at $E_d = 1.30, 2.92,$ and 4.92 MeV. Comparison was made with a direct-capture calculation.

It was decided to restudy the reaction $^9\text{Be}(d, \gamma)^{11}\text{B}$ with improved experimental technique. This was motivated by the lack of data sufficiently accurate to rule out any fine structure in the ground-state excitation function. It was also hoped that extending the excitation-function measurements to include transitions to ^{11}B excited states and measuring a large number of angular distributions might throw more light upon the dominant reaction mechanism. The earlier studies^{21, 22} used NaI(Tl) detectors, massive neutron shielding, and accelerators operating in direct-current mode. Suffert²² used an anticoincidence arrangement involving a liquid scintillator surrounding the NaI(Tl) detector to provide cosmic-ray background rejection; ZBW²¹ subtracted out the flat cosmic-ray spectrum. The most serious experimental problem in the study of this reaction was the large γ -ray counting rate due to the prolific $(d, n\gamma)$ and $(d, p\gamma)$ reactions, and due to neutron capture in the detector. To accumulate a significant number of events, either short runs at high count rates with associated pileup problems, or long runs at lower count rates had to be taken. To overcome these difficulties in the present experiment, a

pulsed and bunched deuteron beam and time-of-flight (TOF) rejection technique was utilized to separate the capture γ rays from unwanted background events.

II. EXPERIMENTAL PROCEDURE

The major experimental improvement in this investigation involved utilization of the pulsed and bunched deuteron beam from the University of Oregon 4-MeV Van de Graaff accelerator to distinguish the desired γ -ray events from those originating from neutrons or cosmic rays. A detailed description of the pulsed ion source has been given elsewhere.²³ A time resolution of 1 nsec (full width at half maximum) on the target was routinely obtained.

The transport, focusing, analyzing, and collimation of the pulsed beam were accomplished in a manner identical to that used with a dc beam and is described elsewhere.²⁴ The target and NaI(Tl) detector were located in a cave composed of 16-in.-thick concrete walls. The beam into this cave passed through two tantalum collimators which were 0.010 in. thick with a 0.188-in.-diam hole in the center. A 7-in.-long cylindrical copper cold-trap, cooled to liquid-nitrogen temperatures, followed. As the target served also as a Faraday cup, the adjacent beam tube was carefully designed with an electron suppressor, as shown in Fig. 1, to ensure proper charge integration. The target was a 0.75-in.-square \times 0.010-in.-thick gold foil with beryllium evaporated onto it *in vacuo*. It was held on a glass target holder by a Viton

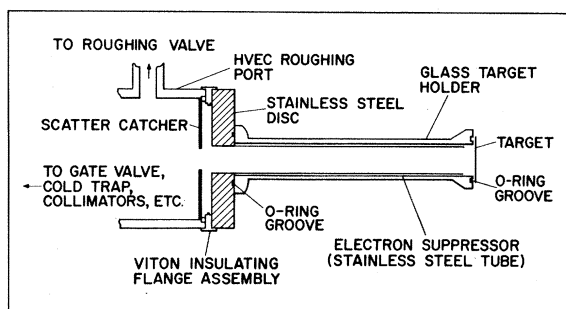


FIG. 1. Schematic diagram of the end of the beam tube and the target holder assembly. The "scatter catcher" was connected electrically from the roughing port to ground through a nanoammeter, collecting particles scattered from the collimators that might otherwise have struck the electron suppressor. The suppressor was held at -300 V and was electrically insulated from the scatter catcher by a standard HVEC Viton insulating flange. The equipotential surface of the electron suppressor ends 0.25 in. from the target and prevents it from "seeing" (by induced charging) the approaching beam pulse until its actual time of arrival.

o-ring and by atmospheric pressure. The target was cooled by a stream of forced air on its back side. A maximum power dissipation of 2.5 W produced no measurable target deterioration. Target thickness was measured at the $E_p = 2.567$ MeV reaction ${}^9\text{Be}(p, \alpha\gamma){}^6\text{Li}$. The natural width of this resonance limited the target thickness determination to an accuracy of $\pm 15\%$.

The γ -ray detector was a 5-in. \times 5-in. NaI(Tl) crystal mounted on an XP1040 photomultiplier tube and located 12.5 in. from the target on a movable arm centered at the target. The γ rays were collimated by a 3-in.-thick lead shield with a truncated conical hole concentric with the cylindrical axis of the crystal. The detector was also shielded by 1.5 in. of lead on the sides. Neutron shielding was accomplished with a 1:1 by weight mixture of lithium carbonate and paraffin, placed concentrically around the target between it and the detector.

TOF technique required the conversion of the time difference between the start of an event in the NaI(Tl) detector and the delayed beam pulse to a pulse height in a time-to-amplitude converter (TAC). Setting an appropriate single-channel-analyzer (SCA) window on the TAC output then permitted rejection of a significant fraction of the events due to neutrons. Additionally, with a 10-nsec window and a 2- μ sec beam-pulse spacing, a cosmic-ray rejection factor of 200:1 was obtained. This was checked experimentally by collecting background counts for 15 h with and without gating.

A block diagram of the electronics used for the TOF neutron and cosmic-ray rejection technique is given in Fig. 2. The linear signal, taken from the 10th dynode of the photomultiplier, was ampli-

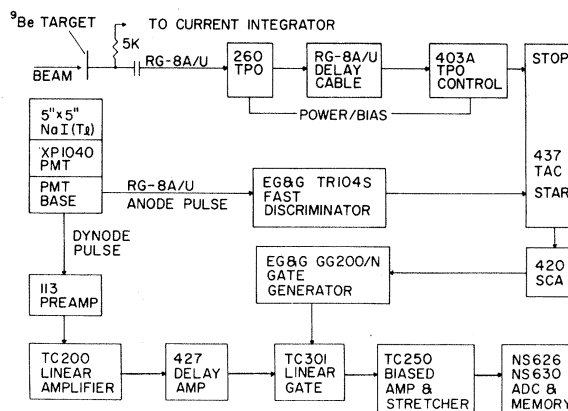


FIG. 2. Block diagram of the electronics arrangement used for the (d, γ) measurements with a pulsed deuteron beam. Details of the timing and adjustment are covered in the text.

fied in the preamplifier and TC-200 amplifier, and sent to the linear gate via a delay amplifier to permit slow timing adjustments. The start pulse for the TAC was provided by the EG&G TR104S fast discriminator which was triggered by the 2-nsec rise-time photomultiplier anode pulse. The stop pulse was furnished by the suitably delayed signal from a time-pickoff unit, initiated by the deuteron beam pulse on the target. Adjustment of the fast timing was done using the reaction $^{19}\text{F}(p, \alpha\gamma)^{16}\text{O}$ which is a convenient source of high-energy γ rays with no neutron background.

The Tennelec TC 200 linear amplifier was operated with double RC differentiation and integration, with short time constants so that the output always returned to the base line within $2 \mu\text{sec}$. Therefore, events from one beam pulse did not interfere with events from the immediately following beam pulse. In the present experiment, where there was some background between pulses, a pulse-pileup problem might be expected to develop. Events separated by $2 \mu\text{sec}$ or more could not pile up. But pileup could occur whenever a background event occurred close to the same time as an event from the most recent pulse, or when a γ ray and slow neutron, both from the same beam pulse, interacted with the detector. The number of these events was found by measuring the time difference between the leading edge of an event pulse, and the point at which it crossed the base line when it was clipped by the double-delay line. At a NaI(Tl) count rate of 34 000/sec, only 2% of the events produced a shift in the crossover point of greater than 15 nsec, thereby implying pileup events. These events were evenly distributed throughout the energy spectrum. From this test, it was decided that no circuitry for pileup rejection was necessary. A problem still remains with summing events which occur whenever two events from the same beam pulse interact with the detector at the same time. Count rates were kept below 50 000 counts/sec to keep the correction for this below 10%.

To find the number of (d, γ) events in a spectrum, it is necessary to know the γ -ray response function of the collimated NaI(Tl) detector so that standard computer stripping procedures can be used. γ -line shapes were established using the following reactions: $^{27}\text{Al}(p, \gamma)^{28}\text{Si}$ for an 11.14-MeV γ ray, $^{11}\text{B}(d, n\gamma)^{12}\text{C}$ for a 15.11-MeV γ ray, and $^{11}\text{B}(p, \gamma)^{12}\text{C}$ for an 18.71-MeV γ ray. Line shapes for intermediate γ rays were then computed using a quadratic interpolation. A horizontal line was used for the low-energy portion of these spectra. This extrapolation yielded an estimated $\pm 20\%$ error to the absolute cross-section determination. The absolute differential cross section was cal-

culated from the expression

$$\sigma = \frac{A - B}{\epsilon TC f ND \Omega} \quad (1)$$

In this equation, A is the number of detected events for a given γ ray stripped from the γ spectrum, and B is the number of background events in the peak. Both A and B were corrected for ADC dead time. T is the transmission coefficient for a γ ray of energy E passing through the intervening material from target to NaI(Tl) detector. $\epsilon = \epsilon(E_\gamma)$ is the total γ -ray efficiency of the NaI(Tl) detector, Ω is the detector solid angle in steradians, D takes into account target deterioration (none was observed), N is the number of target nuclei/cm², f is the correction for the TAC dead time,²⁵ and C is the number of deuterons striking the target during the time the SCA window was open.

Angular-distribution measurements were taken at 0, 30, 55, 75, 95, 110, and 130° at low energies and at 0, 30, 55, 75, 90, 105, and 120° at higher energies. Anisotropy of the neutron absorbing material and lack of centering of target and beam spot over the rotation axis of the detector were measured using the $^{19}\text{F}(p, \alpha\gamma)^{16}\text{O} = 6.13$ -MeV γ ray at the $E_p = 936$ -keV resonance, which is isotropic to $\pm 0.3\%$.²⁶ Small corrections of the order of 1–6% were necessary in the region from 75–95° where the gold target backing became a disproportionately large component of the attenuating materials.

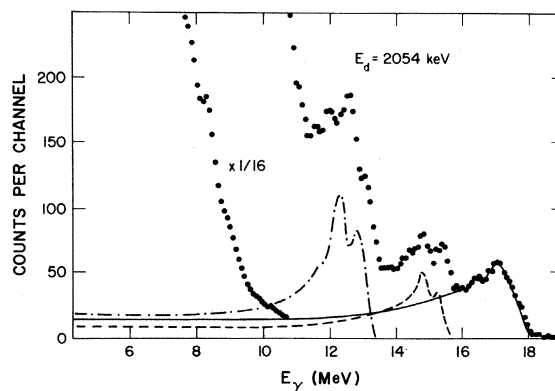


FIG. 3. Sample (d, γ) data obtained with ^9Be target and pulsed and bunched deuteron beam. The 5-in. \times 5-in. NaI(Tl) detector was positioned 12.5 in. from the target at 55° to the incident deuterons. The solid curve shows the fit obtained to the ground-state transition with the γ -ray fitting program. The dashed curve is the fit for the first-excited-state transition while the dot-dashed curve is that for the transition to the combined second and third excited states of ^{11}B .

III. RESULTS

A typical (d, γ) spectrum obtained with the 5-in. \times 5-in. NaI(Tl) detector using the pulsed deuteron beam is shown in Fig. 3. This spectrum was obtained at $E_d = 2.054$ MeV, and was smoothed once with a three-channel average. The peaks of the γ rays corresponding to transitions of 17.500 and 15.376 MeV to the ground and first excited states, respectively, are easily seen. The γ ray for the transition to the combined second and third excited states sits on the edge of the rapidly rising background, which is principally due to summing of low-energy γ rays. The solid and dashed curves show fits obtained with the γ -ray stripping program to the three separate peaks.

Excitation-function measurements were taken at 55° to the beam direction over the incident-deuteron energy range of 0.56–3.56 MeV, and cross sections were calculated with Eq. (1). In addition, angular distributions were measured at 21 different deuteron energies spread throughout this deuteron energy interval. The angular distributions were fitted to a polynomial $A_0 + A_1 P_1(\cos\theta) + A_2 P_2(\cos\theta)$. The ratio of A_1 to A_0 for the ground-state transition was less than 5% at all times; the total cross-section data obtained from the angular distributions were then combined with $4\pi d\sigma/d\Omega(55^\circ)$ from the excitation-function measurements to give the total-cross-section plot shown in Fig. 4. The errors shown on the figure are relative. In addition, there is a possible $\pm 35\%$

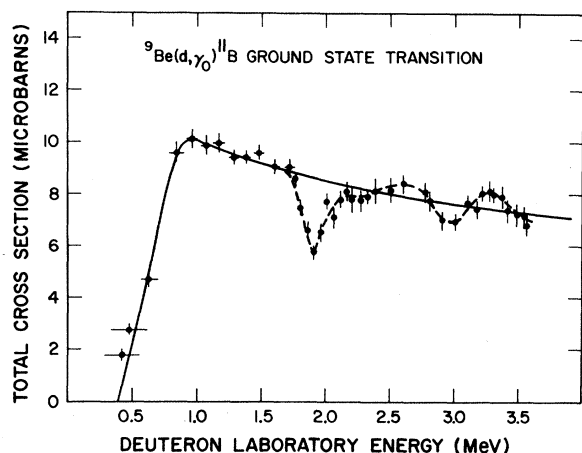


FIG. 4. Excitation function for the ground-state γ -ray transition in the reaction ${}^9\text{Be}(d, \gamma){}^{11}\text{B}$. Data points were obtained both from angular-distribution measurements and from runs at 55° to the incident beam as described in the text. Horizontal bars on the data points show the energy loss of the deuteron in passing through the target. The solid curve is meant to represent the over-all data behavior neglecting the resonance structure. The dashed curve is drawn through the actual data points.

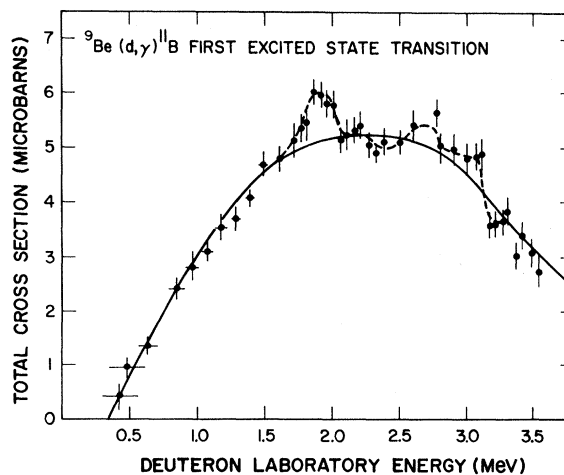


FIG. 5. Excitation function for the γ -ray transition to the ${}^{11}\text{B}$ first excited state in the reaction ${}^9\text{Be}(d, \gamma){}^{11}\text{B}$. Data points were obtained both from angular-distribution measurements and from runs at 55° to the incident beam as described in the text. Horizontal bars on the data points show the energy loss of the deuteron in passing through the target. The solid curve is meant to represent the over-all data behavior neglecting the resonance structure. The dashed curve is drawn through the actual data points.

error in the absolute cross-section scale, due mainly to a lack of knowledge of the low-energy detector response and of the target thickness. The maximum cross section of $10.1 \pm 3.5 \mu\text{b}$ occurs near $E_d = 960$ keV. The solid line depicts

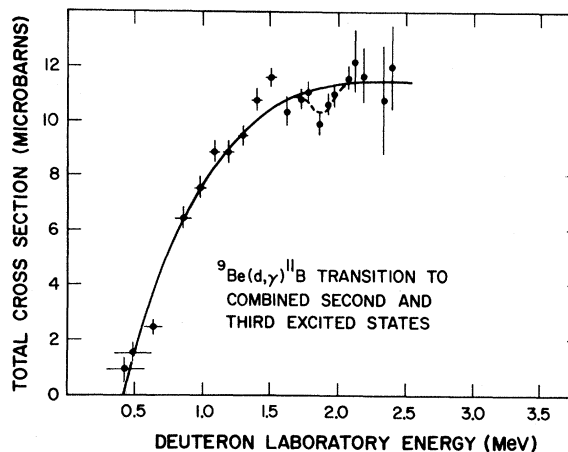


FIG. 6. Excitation function for the γ -ray transitions to the combined second and third excited states in ${}^{11}\text{B}$ in the reaction ${}^9\text{Be}(d, \gamma){}^{11}\text{B}$. Data points were obtained from runs at 55° to the incident beam as described in the text. Horizontal bars on the data points show the energy loss of the deuteron in passing through the target. The solid curve is meant to represent the over-all data behavior neglecting the resonance structure. The dashed curve is drawn through the actual data points.

the smooth over-all shape of the excitation function, ignoring fluctuations. The excitation function shows definite evidence of fine structure.

The structure observed in the ground-state excitation function is confirmed by the excitation function for the γ -ray transition to the ^{11}B first excited state at 2.124 MeV. Figure 5 shows cross-section behavior, again obtained by combining the 55° excitation-function results with those from the angular-distribution measurements. As above, there is a definite fine structure superimposed on the smooth over-all cross-section behavior. The data for the γ -ray transitions to the combined second and third excited states of ^{11}B at 4.44 and 5.019 MeV are shown in Fig. 6. These data terminate at $E_d = 2.38$ MeV, as these transitions become obscured by the background at higher energies. The presence of structure near 2.0 MeV is clearly indicated. The uncertainty in the absolute cross sections for these two excitation functions is also $\pm 35\%$.

The resonance structure present in Figs. 4–6 has been analyzed by a simple graphical procedure.²⁷ It was felt that this method is sufficiently precise to establish the basic resonance parameters to an accuracy justified by the data. The results are presented in Table I. The evidence for the resonances at 1.98 ± 0.05 and 3.12 ± 0.05 MeV appears to be quite good. The former appears in all three excitation functions and the latter resonance shows up in both the ground- and first-excited-state excitation functions.

Typical examples of the angular-distribution data, along with the corresponding least-squares Legendre polynomial fits to $A_0 + A_1P_1(\cos\theta) + A_2P_2(\cos\theta)$ for the γ -ray transitions to the ground and first excited states for deuteron energies of 2.005 and 3.106 MeV are presented in Fig. 7. Finite-geometry corrections to the coefficients were small and have not been made. Least-squares fits were also done with other combinations of Legendre polynomials, including one with all terms through $P_3(\cos\theta)$. Examination of the χ^2 results showed that the combination including A_0 , A_1 , and A_2 was both needed and sufficient.

Angular-distribution measurements for the transition to the ground state in the reaction $^9\text{Be}(d, \gamma)\text{-}^{11}\text{B}$ at deuteron energies in the range of this study

TABLE I. Analysis of fine-structure resonances.

Resonance energy (MeV)	Resonance width (keV)	^{11}B excitation energy (MeV)
1.98 ± 0.05	225 ± 50	17.44 ± 0.05
3.12 ± 0.05	320 ± 100	18.37 ± 0.05

were made at 1.175 MeV by ZBW,²¹ and at 1.30 and 2.92 MeV by Suffert.²² ZBW²¹ calculated a fit to their distributions corresponding to $A_0P_0(\cos\theta) + A_2P_2(\cos\theta)$, where their value of A_2/A_0 is -0.09 ± 0.11 , indicating no statistically significant deviation from isotropy. The similar ratio measured in the present study at 1.175 MeV gives -0.14 ± 0.04 , in agreement with the earlier result as to magnitude and sign, but in definite disagreement with their conclusion of isotropy. Agreement between the angular-distribution fits of Suffert²² and the present results is good, particularly for the 1.30-MeV measurement, although no errors were quoted in the earlier work. For example, at 1.30 MeV, Suffert²² obtained $w(\theta) = 1 + 0.18P_1(\cos\theta) - 0.18P_2(\cos\theta)$, whereas the present measurements give $1 + (0.05 \pm 0.02)P_1(\cos\theta) - (0.17 \pm 0.03) \times P_2(\cos\theta)$ for the angular distribution measured at 1.28 MeV.

The behavior of A_1/A_0 and A_2/A_0 for the ground- and first-excited-state transitions presented in Figs. 8 and 9, respectively, as a function of deuteron energy. The ground-state results show little tendency to forward peaking, as the A_1/A_0 ratio is practically zero throughout the entire range of deuteron energies covered in the present experiment. The A_2 coefficient is always negative, indicating an anisotropic angular distribution symmetric about and with a maximum at 90° . The behavior near the resonances at 2.0 and 3.1 MeV is not marked. Legendre polynomial fits for the transition to the first excited state shown in Fig. 9 display interesting behavior at both resonances. At energies below 2.0 MeV, the angular distribution is forward peaked, while at 2.1 MeV it becomes symmetric about 90° . At the location of the upper resonance, the angular distribution becomes very strongly forward peaked and very anisotropic, whereas at slightly lower energies, it is symmetric about 90° .

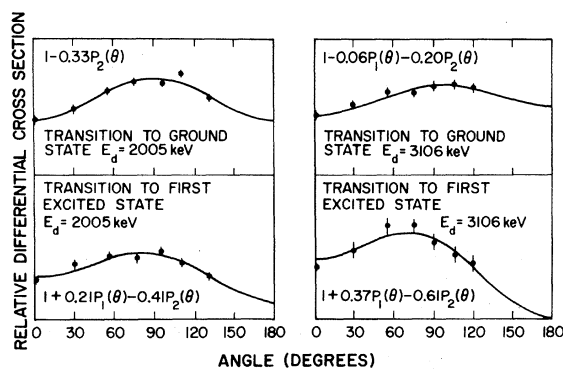


FIG. 7. Typical examples of angular-distribution data. The solid curve represents a least-squares fit to $A_0 + A_1P_1(\cos\theta) + A_2P_2(\cos\theta)$, with A_0 normalized to unity.

IV. DISCUSSION

The present experimental technique using a pulsed deuteron beam has resulted in a considerable improvement over past methods of study of the (d, γ) reaction. The TOF technique, which permits the rejection of a large fraction of neutron-capture events from the spectra, has allowed operation at high counting rates with a subsequent reduction in the counting period needed for data accumulation, and has afforded a 200:1 reduction in the cosmic-ray background. This large reduction in unwanted background has allowed us to measure excitation functions corresponding to three different γ -ray transitions, which could not have been done without the improved technique.

As shown in Figs. 4-6, and contrary to the earlier work on this reaction,^{21, 22} the excitation functions have a fine structure superimposed on the smooth part of the cross section. From Table I, the energies of these resonances have tentatively been assigned to 1.98 ± 0.05 and 3.12 ± 0.05 MeV. The inability to observe these resonances in the previous (d, γ) work was undoubtedly due to the poorer statistical quality of the earlier measurements. These resonances correspond to excitation energies in ${}^{11}\text{B}$ of 17.44 ± 0.05 and 18.37 ± 0.05 MeV. If we assume $E1$ transitions, these results imply a spin and parity of either $\frac{1}{2}^+$ or $\frac{3}{2}^+$ for these

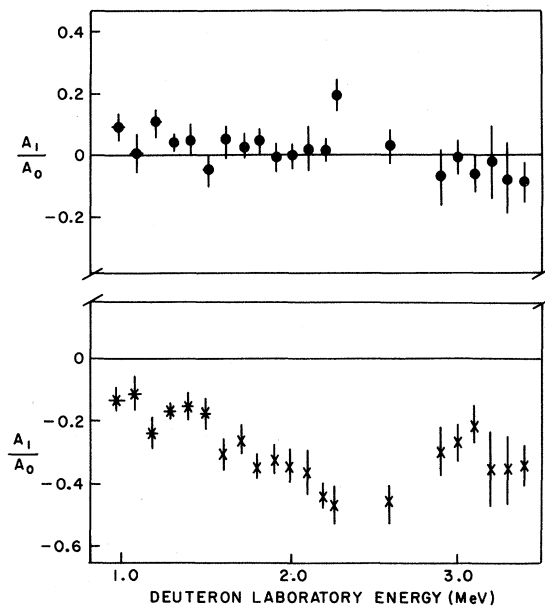


FIG. 8. Plots of the Legendre polynomial coefficients obtained from the angular-distribution measurements as a function of the incident deuteron energy for the γ -ray transition to the ground state of ${}^{11}\text{B}$.

excited states in ${}^{11}\text{B}$.

The resonance corresponding to a ${}^{11}\text{B}$ excitation energy of about 17.44 MeV is probably the same as the level at 17.53 ± 0.03 MeV.²⁸ This level was found in the reaction ${}^7\text{Li}(\alpha, n){}^{10}\text{B}$ ²⁹ as a narrow peak in the excitation function. This level was also found as a small dip in the ${}^9\text{Be}(d, p){}^{10}\text{Be}^*$ 3.37-MeV γ -ray excitation function³⁰ and was observed weakly in the ${}^{10}\text{B}(n, \alpha){}^7\text{Li}$ excitation function.³¹

A Q value of -34.3 ± 0.8 MeV was obtained for the ejection of a $1s_{1/2}$ proton out of ${}^{12}\text{C}$ in the reaction ${}^{12}\text{C}(p, 2p){}^{11}\text{B}$,³² corresponding to an ${}^{11}\text{B}$ excitation of 18.3 ± 0.8 MeV and a spin and parity of $\frac{1}{2}^+$. Since the lifetime of the $1s_{1/2}$ hole state is very short, this level is very broad. An experimental width of about 9 MeV is obtained,³² which has been confirmed by a theoretical calculation.³³ This state is probably spread out over many ${}^{11}\text{B}$ compound-nuclear levels. It is then possible that the resonances in the (d, γ) reaction might correspond to fine-structure states of $(1s_{1/2})^{-1}$ type. If so, they should have γ -ray transition strengths of the order of a single-particle unit corresponding to a $1p_{3/2}$ to $1s_{1/2}$ transition. At present, no information about Γ_d is available, so that Γ_γ cannot be evaluated. The narrowness of these levels

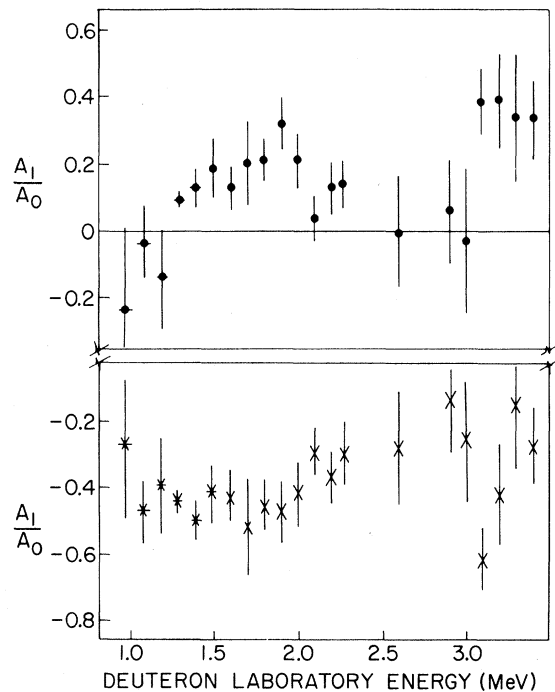


FIG. 9. Plots of the Legendre polynomial coefficients obtained from the angular-distribution measurements as a function of the incident deuteron energy for the γ -ray transition to the first excited state of ${}^{11}\text{B}$.

would then be due to the small strength of each of these fine-structure resonances.

The excitation of a $\frac{1}{2}^+$ state in the present experiment can be explained with the aid of Fig. 10. Figure 10(a) shows the ^9Be ground state with its $s_{1/2}$ shell filled. When the incoming deuteron has the proper center-of-mass energy it interacts with the nucleons of the ^9Be nucleus in such a manner as to raise a proton from the $s_{1/2}$ state up to the $p_{3/2}$ state. At the same time, the neutron and proton of the deuteron fill the $p_{3/2}$ shell as shown in Fig. 10(b). The excited ^{11}B nucleus then decays via an $E1$ transition to the ground-state configuration shown in Fig. 10(c) by a single-particle transition of a $p_{3/2}$ proton to the hole in the $1s_{1/2}$ shell. This type of a core excited state is certainly not the only one possible. Another would be the core-polarization indirect transition, where the projectile excites the target with the giant resonance as the dominant excitation.

The angular distributions for the ground-state transition are essentially symmetric about 90° over the entire deuteron energy range, but are definitely anisotropic. The angular distributions for the transition to the first excited state of ^{11}B are both anisotropic and forward-peaked. The symmetry of the angular distributions for the ground-state transition does not necessarily differentiate between the compound-nuclear and direct-capture

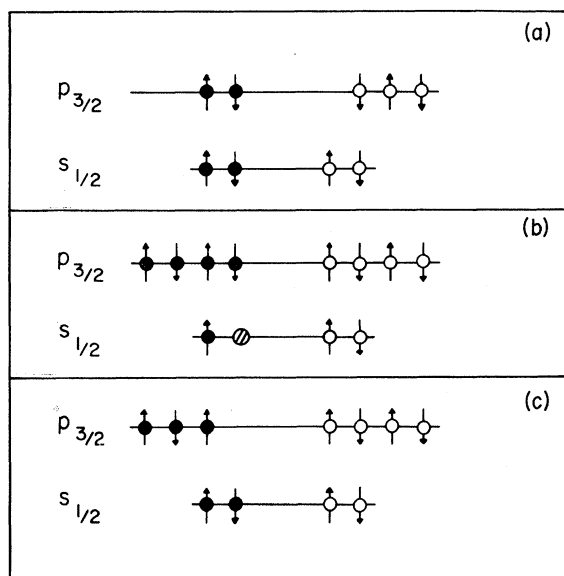


FIG. 10. A schematic diagram of the filling of the orbits in ^{11}B for the interpretation of the resonance structure in the reaction $^9\text{Be}(d, \gamma)^{11}\text{B}$ suggested in the text. (a) shows the ^9Be ground-state configuration; (b) shows the ^{11}B configuration immediately after capture of a deuteron and excitation of an $s_{1/2}$ proton; and (c) shows the ^{11}B ground-state configuration.

mechanisms.^{18,34} Compound-nuclear distributions, while usually isotropic, need only be symmetric about 90° . For a direct-capture mechanism the peaking of the ground- and first-excited-state distributions at 90° would imply a sum of one-step and two-step processes.¹⁸ For a one-step process $w(\theta) \sim \sin^2\theta$ and for the two-step process $w(\theta) \sim 1 + \cos^2\theta$, with an incoherent sum giving a symmetric distribution. The forward peaking could then arise from a coherent sum of the one- and two-step processes. Finally, the forward peaking could also be explained as arising from an $E2$ contribution to the γ -ray transition.

One certain conclusion is that *if* the dominant mechanism for the reaction is a direct-capture process, then the peaking at 90° in the ground-state transition (which probably has no $E2$ contribution) implies that the one-step process is quite important. This can arise for an $E1$ transition in a light nucleus where the $(N-Z)/A$ weighting is not too significant. For heavier self-conjugate nuclei this term should not be important. The most probable conclusion from the angular-distribution results, in our opinion, is that the dominant reaction mechanism is a direct-capture process with both the one- and two-step terms participating with approximately equal strengths.

In addition to the fine-structure resonances which show up in all three excitation functions, there is a remarkable similarity between them as to their over-all behavior with deuteron energy. ZBW²¹ first noticed this similarity, although they concluded that the intensity ratios as a function of energy for the ground, first, and combined second and third excited states were constant with observed values of

$$I_0 : I_1 : I_{2+3} = 1 : (0.30 \pm 0.08) : (0.78 \pm 0.15).$$

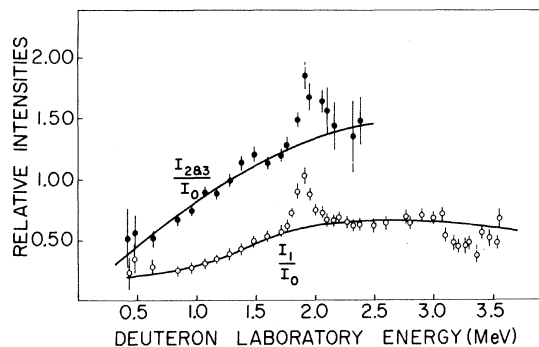


FIG. 11. Intensities of the γ -ray transitions to the combined second and third excited states and to the first excited state divided by the ground-state transition plotted as a function of deuteron energy. The solid curves are meant to represent the over-all data behavior neglecting the resonance structure.

The excitation-function measurements of the present study have been combined to obtain these intensity ratios as a function of deuteron energy and are plotted in Fig. 11. It is apparent that there is some change with energy, particularly for the transition to the combined second and third excited states. The fluctuations at the two resonances are again apparent. The slight energy dependence to the smooth part of the I_1/I_0 ratio is shown by the variation between 0.3 and 0.6. The energy dependence of I_{2+3}/I_0 is more marked as this rises from about 0.6 at low energies to about 1.5. Assuming single-particle transitions of $E1$ type, ZBW²¹ calculated a ratio of 1:0.33:0.93 for p -wave deuteron capture. They concluded that the ${}^{11}\text{B}$ giant dipole resonance, centered at 23 MeV, was not influential in the reaction mechanism, as the ground-state transition would be even more favored. If a semidirect (collective) capture process were important it would be the giant dipole resonance of the target nucleus, ${}^9\text{Be}$, which would enter as an intermediate state in the capture process.⁸⁻¹⁰ The present results are not inconsistent with this picture, as the intensity ratios as a function of energy tend to flatten out for I_1/I_0 about 2 MeV above the peak for the ground-state γ ray, and I_{2+3}/I_0 peaks at an even higher energy. Furthermore, both ratios rise with energy to values nearly a factor of 2 above the corresponding single-particle prediction. If this process were important, it would imply for the two-step process that the incoming deuteron first undergoes a stripping process to the various ${}^{11}\text{B}$ states, with excitation of the giant dipole resonance as an intermediate step which would thereby enhance the radiative-deuteron-capture cross section over the simple direct-capture value.

Further evidence for the reaction mechanism being that of a direct-capture process comes from the very smooth behavior of the excitation functions except for the two fine-structure resonances superimposed. This is indicated by the solid lines on Figs. 4-6. If the explanation of this over-all cross-section behavior were a broad compound-nucleus level, the peak location and width of all three excitation functions should be the same, in obvious contradiction with the experimental results. The behavior of the (d, γ) cross section near threshold has a shape which is in good ac-

cord²¹ with that predicted from the ${}^{12}\text{C}(\gamma, d)$ calculation¹⁸ appropriately modified for the extension to ${}^{11}\text{B}$ and invoking detailed balance. A similar statement can be made for the behavior of the ground-state excitation function at deuteron energies above the cross-section maximum. Comparison with both the predictions of Joccoz and Zang²² and Madsen and Henley¹⁸ shows agreement both in energy dependence and magnitude. If the explanation of the over-all excitation-function behavior were a broad compound-nucleus resonance, the forward peaking in the first-excited-state angular distributions could possibly arise from interference between the broad and the fine-structure resonances, but the broad and fine-structure states would have to have opposite parities.

As noted in the Introduction, the radiative-deuteron-capture reaction has not been sufficiently studied as yet for a definite conclusion about the dominant reaction mechanism to be made. Results from the reaction $\text{D}(d, \gamma){}^4\text{He}$ ¹⁴ and from the capture of energetic deuterons by isotopes of uranium¹⁵ favor a direct-capture mechanism. On the other hand, statistical theory calculations have been used to explain the activation measurement on ${}^{30}\text{Si}$ and ${}^{138}\text{Ba}$,¹⁶ and on ${}^{54}\text{Cr}$, ${}^{58}\text{Ni}$, and ${}^{64}\text{Zn}$.¹⁷ The authors of the last measurements also normalized their ${}^{58}\text{Ni}(d, \gamma)$ results to $[(N-Z)/A]^2$ and checked whether or not the results for ${}^{64}\text{Zn}(N-Z=4)$ and ${}^{54}\text{Cr}(N-Z=6)$ were proportional to the deuteron penetration factor and to $[(N-Z)/A]^2$. They did not get the right proportionality. This procedure is most probably invalid, however, since the two-step electric dipole direct-capture process is most probably dominant for nonlight nuclei.¹⁸ The results of the present experiment give strong support for the direct-capture mechanism. More experimental information on other nuclei is needed to positively identify the dominant reaction mechanism.

ACKNOWLEDGMENTS

We would like to acknowledge useful discussions about the electronics with Professor H. W. Lefevre. D. Hendricks assisted with some of the data taking. Professor V. Madsen made many useful suggestions concerning the interpretation in terms of direct-capture theory.

†Work supported in part by the U. S. Atomic Energy Commission.

*Present address: Sandia Corporation, Livermore, California.

¹A. M. Lane and J. E. Lynn, Nucl. Phys. **11**, 646 (1959).

²I. Bergqvist, D. Drake, and D. K. McDaniels, Phys. Rev. Letters **27**, 269 (1971).

³B. L. Cohen, Phys. Rev. **100**, 206 (1955).

⁴B. Kursunoglu, Phys. Rev. **105**, 1846 (1957).

⁵F. Beck, Physica **22**, 1164 (1956).

- ⁶A. M. Lane, Nucl. Phys. 11, 625 (1959).
- ⁷P. J. Daly, J. R. Rook, and P. E. Hodgson, Nucl. Phys. 56, 331 (1964).
- ⁸C. F. Clement, A. M. Lane, and J. R. Rook, Nucl. Phys. 66, 273, 293 (1965).
- ⁹A. A. Lushnikov and D. F. Zaretsky, Nucl. Phys. 66, 35 (1965).
- ¹⁰G. E. Brown, Nucl. Phys. 57, 339 (1964).
- ¹¹D. Drake, S. L. Whetstone, and I. Halpern, to be published.
- ¹²I. Bergqvist, D. Drake, and D. K. McDaniels, to be published.
- ¹³R. V. Carlson and P. J. Daly, Nucl. Phys. A102, 177 (1967).
- ¹⁴W. E. Meyerhof, W. Feldman, S. Gilbert, and W. O'Connell, Nucl. Phys. A131, 489 (1969).
- ¹⁵R. M. Lessler, W. M. Gibson, and R. A. Glase, Nucl. Phys. 81, 401 (1966).
- ¹⁶F. W. Pement and R. L. Wolke, Nucl. Phys. 86, 417 (1966).
- ¹⁷J. H. Carver and G. A. Jones, Nucl. Phys. 11, 400 (1959); 24, 607 (1961).
- ¹⁸V. A. Madsen and E. M. Henley, Nucl. Phys. 33, 1 (1962).
- ¹⁹V. P. Chizkov, A. P. Komar, L. A. Kulchitsky, A. V. Kulikov, E. D. Makhnovsky, and Yu. M. Volkov, Nucl. Phys. 34, 562 (1962).
- ²⁰H. R. Allan and N. Sarma, Proc. Phys. Soc. (London) 68, 535 (1955).
- ²¹B. Ziegler, W. Buss, and H. Wäffler, Nucl. Phys. 83, 145 (1966).
- ²²M. Suffert, Nucl. Phys. 75, 226 (1966).
- ²³W. R. Wylie, R. M. Bahnsen, and H. W. Lefevre, Nucl. Instr. Methods 79, 245 (1970).
- ²⁴E. F. Gibson, K. Battleson, and D. K. McDaniels, Phys. Rev. 172, 1004 (1968).
- ²⁵K. Battleson and D. K. McDaniels, Nucl. Instr. Methods 91, 295 (1971).
- ²⁶H. Martin, W. Fowler, C. Lauritsen, and T. Lauritsen, Phys. Rev. 106, 1260 (1957).
- ²⁷H. Seitz, Nucl. Instr. Methods 86, 157 (1970).
- ²⁸F. Ajzenberg-Selove and T. Lauritsen, Nucl. Phys. A114, 1 (1968).
- ²⁹M. K. Mehta, W. E. Hunt, H. S. Plendl, and R. H. Davis, Nucl. Phys. 48, 90 (1963).
- ³⁰J. H. McCrary, T. W. Bonner, and W. A. Ranken, Phys. Rev. 108, 392 (1957).
- ³¹E. A. Davis, F. Gabbard, T. W. Bonner, and R. Bass, Nucl. Phys. 27, 448 (1961).
- ³²M. Riou, Rev. Mod. Phys. 37, 375 (1965); H. Tyrén, S. Kullander, O. Sundberg, R. Ramachandran, P. Isaccson, and T. Berggren, Nucl. Phys. 79, 321 (1966).
- ³³H. S. Köhler, Nucl. Phys. 88, 529 (1966).
- ³⁴H. Gutfreund and G. Rakavy, Nucl. Phys. 79, 257 (1966).